Mass Spectral Analysis of Asphaltenes. I. Compositional Differences between Pressure-Drop and Solvent-Drop Asphaltenes Determined by Electrospray Ionization Fourier Transform Ion Cyclotron Resonance Mass Spectrometry

Geoffrey C. Klein,[†] Sunghwan Kim, Ryan P. Rodgers,[†] and Alan G. Marshall*,[†]

National High Magnetic Field Laboratory, Florida State University, 1800 East Paul Dirac Drive, Tallahassee, Florida 32310-4005

Andrew Yen and Sam Asomaning

Baker Petrolite, 12645 West Airport Boulevard, Sugar Land, Texas 77478

Received January 13, 2006. Revised Manuscript Received June 8, 2006

Asphaltenes are typically defined by their solubility in benzene and insolubility in pentane or heptane. They are believed to exist in petroleum crude oil as a colloidal suspension, stabilized by surface-adsorbed resins. Their normal equilibrium under reservoir conditions may be disrupted during production by pressure reduction, crude oil chemical composition changes, introduction of miscible gases and liquids, and mixing with diluents and other oils, as well as by acid stimulation, hot oiling, and other oilfield operations. Electrospray ionization preferentially ionizes polar N-, S-, and O-containing compounds, and its combination with ultrahigh-resolution Fourier transform ion cyclotron resonance mass spectrometry makes a powerful tool for the compositional analysis of petroleum-derived materials such as asphaltenes. In this work, we compare the compositional differences between heptane-precipitated asphaltenes and asphaltenes collected by live oil depressurization. Negative- and positive-ion electrospray yield the acidic and basic species, respectively. We find that the heptane-precipitated asphaltenes contain higher double bond equivalents (number of rings plus double bonds) compared to the asphaltenes induced by pressure drop. On the other hand, the pressure-drop product exhibits a higher abundance of species containing sulfur. Thus, the solubility criterion for asphaltenes defines a significantly different chemical composition than the (more field-relevant) pressure-drop criterion.

Introduction

Crude oil is one of the most complex mixtures in the world and is composed of thousands of species that define its chemical and physical properties. The constituents of crude oils are typically classified by solubility: saturates, aromatics, resins, and asphaltenes (SARA).[1−3] SARA fractionation starts with removal of asphaltenes by precipitation with a saturated hydrocarbon (e.g., heptane). Subsequent elution with a series of increasingly polar solvents as the mobile phase yields saturates (eluted with a nonpolar solvent such as hexane), followed by the elution of aromatics with toluene, and the resins are separated with a more polar solvent. Here, we focus on the asphaltenes because they can generate major problems in production, and because it is important to establish the degree of correspondence between laboratory and field definitions of asphaltenes.

Problems associated with asphaltene precipitation and deposition have been widely reported in the petroleum production and processing industry.[4−7] Asphaltene precipitation and subsequent deposition in production tubing and topside facilities impose significant cost penalties to crude oil production. Some of the parameters reported to affect asphaltene precipitation/deposition include pressure, composition, and temperature. A primary criterion to study asphaltene precipitation/deposition for upstream operation is live oil depressurization,[8,9] to determine the onset pressure for asphaltene precipitation and the quantity of asphaltenes precipitating out of solution and depositing on the cell wall.

* To whom correspondence should be addressed. E-mail: marshall@magnet.fsu.edu.

[†] Member of the Department of Chemistry, Florida State University, Tallahassee, Florida.

(1) Jewell, D. M.; Weber, J. H.; Bunger, J. W.; Plancher, H.; Latham, D. R. Ion-Exchanger, Coordination and Adsorption of Chromatographic Separation of Heavy Petroleum Distillates and Analysis of Hydrocarbon Fractions. *Erdoel Kohle, Erdgas, Petrochem.* **1973**, *26* (10), 580.

(2) McLean, J. D.; Kilpatrick, P. K. Comparison of precipitation and extrography in the fractionation of crude oil residua. *Energy Fuels* **1997**, *11* (3), 570−585.

(3) Suatoni, J. C.; Swab, R. E. Rapid Hydrocarbon Group-Type Analysis by High-Performance Liquid-Chromatography. *J. Chromatogr. Sci.* **1975**, *13* (8), 361−366.

(4) Duyck, C.; Miekeley, N.; da Silveira, C. L. P.; Szatmari, P. Trace element determination in crude oil and its fractions by inductively coupled plasma mass spectrometry using ultrasonic nebulization of toluene solutions. *Spectrochim, Acta, Part B* **2002**, *57* (12), 1979−1990.

(5) Park, S. J.; Mansoori, G. A. Aggregation and Deposition of Heavy Organics in Petroleum Crudes. *Energy Sources* **1988**, *10* (2), 109−125.

(6) Taylor, S. E. Use of Surface-Tension Measurements to Evaluate Aggregation of Asphaltenes in Organic-Solvents. *Fuel* **1992**, *71* (11), 1338−1339.

(7) Thawer, R.; Nicholl, D. C. A.; Dick, G. Asphaltene Deposition in Production Facilities. *SPE Prod. Eng.* **1990**, 475−480.

(8) Asomaning, S.; Gallagher, C. In *High-Pressure Asphaltene Deposition Technique for Evaluating the Deposition Tendency of Live Oil and Evaluating Inhibitor Performance*, Preprints of The Second International Conference On Petroleum and Gas-Phase Behavior and Fouling, Copenhagen, Denmark, August 26−31, 2000.

(9) Hammami, A.; Phelps, C. H.; Monger-McClure, T.; Little, T. M. Asphaltene precipitation from live oils: An experimental investigation of onset conditions and reversibility. *Energy Fuels* **2000**, *14* (1), 14−18.

10.1021/ef0600199 CCC: $33.50
Published on Web 07/20/2006

In the laboratory, asphaltenes are conveniently defined by solubility as those compounds in "dead" oil (i.e., oil at atmospheric pressure) that are insoluble in hexane (IP 143 and ASTM 6560). In the field, asphaltenes (precipitation/deposition) are induced by pressure reduction as crude oil is produced from the reservoir pressure to the surface. Structurally, asphaltenes are typically thought of as complex mixtures of heteroatom-rich polycyclic hydrocarbons. More specifically, asphaltenes comprise condensed aromatic and naphthenic molecules of molar masses up to ~2 000 Da.[10,11] They are also the most polar fraction in crude oil and comprise much of the heteroatom (N, S, and O) and metal (Ni and V) content of heavy oils. Because of its inherent compositional complexity, the actual chemical structure of asphaltenes is difficult to define with existing analytical tools.

Here, we apply microelectrospray ionization[12] Fourier transform ion cyclotron resonance (FT-ICR) mass spectrometry (ESI FT-ICR MS)[13] to two asphaltenes samples collected from C_7 precipitation and live oil depressurization experiments, from the same well. A previous study of these two asphaltenes was unable to determine detailed class (heteroatom content), type (aromatic character), and alkylation pattern.[14] The present results, therefore, offer the first detailed chemical composition comparison of dead oil asphaltenes deposit and live oil asphaltenes deposit extracted from the same crude oil. FT-ICR mass spectrometry affords high mass resolving power ($m/\Delta m_{50\%} > 300\,000$, in which $\Delta m_{50\%}$ denotes mass spectral peak full width at half-height) and high mass accuracy, <1 ppm, for the unambiguous assignment of elemental composition to thousands of components per mass spectrum. ESI FT-ICR MS has been successfully applied to complex mixtures such as crude oil[15−21] and coal.[22−24] Such results have laid the groundwork for the new field of "petroleomics",[25,26] namely, the correlation (and, ultimately, prediction) of the properties and behavior of petroleum and its distillates from their detailed chemical compositions. Positive- and negative-ion electrospray serve to reveal the basic and acidic components, respectively, of the two samples. Accurate mass measurement generates elemental compositions ($C_cH_hN_nO_oS_s$) of thousands of components of each of the two differently defined asphaltene samples. From those elemental compositions, the samples may be further characterized according to the relative abundance distributions for different heteroatom-containing classes (i.e., $N_nO_oS_s$), rings plus double bonds (double bond equivalents, or DBE) to reveal the degree of aromaticity for each compound, and carbon distribution (to reveal the extent of alkylation of aromatic cores). It thus becomes possible to determine, in unprecedented detail, the differences in chemical composition of asphaltenes defined by solubility vs pressure-drop (P-drop) method. The differences turn out to be substantial.

Materials & Methods

P-Drop Asphaltenes. The samples were collected downhole with a pressure-compensated single-phase sampler (SRS) by Oilphase Schlumberger according to standard industry practice. The experiment was performed with a high-pressure pressure−volume−temperature (PVT) cell equipped with a near-infrared laser-based solids detection system described previously.[8]

The oil was equilibrated on a rocker to a single-phase fluid at the bottomhole temperature and an initial pressure of 12 000 psia for 1 week. The previously conditioned oil (45 mL) was charged into the PVT cell, by use of a positive displacement pump. The temperature of the cell and its contents was kept at 138 °C and 12 000 psia for 8 h to further condition the oil inside the cell. A baseline transmittance of the laser was initially established. Depressurization consisted of stepping down the pressure in 100 psia decrements. A relaxation period of 7 min between pressure steps allowed the transmittance of the laser to equilibrate. As the pressure on the live oil decreased, it became less dense, thus allowing more light to be transmitted through it. The intensity of transmitted light increases until asphaltenes in the oil start to precipitate, and then it decreases. The point at which the transmittance starts to decrease is the onset pressure of asphaltene precipitation and corresponds to the pressure at which asphaltene precipitation begins in the wellbore. After the oil was depressurized, the asphaltene deposits on the cell walls, on the mixer, and endcap were washed off with toluene. The toluene was evaporated, and the solids were analyzed gravimetrically. The fraction of asphaltenes that precipitated but that did not stick to a surface was filtered out

(10) Groenzin, H.; Mullins, O. C. Molecular size and structure of asphaltenes from various sources. *Energy Fuels* **2000**, *14* (3), 677−684.
(11) Groenzin, H.; Mullins, O. C. Asphaltene molecular size and structure. *J. Phys. Chem. A* **1999**, *103* (50), 11237−11245.
(12) Emmett, M. R.; White, F. M.; Hendrickson, C. L.; Shi, S. D.-H.; Marshall, A. G. Application of Micro-Electrospray Liquid Chromatography Techniques to FT-ICR MS to Enable High Sensitivity Biological Analysis. *J. Am. Soc. Mass Spectrom.* **1998**, *9*, 333−340.
(13) Marshall, A. G.; Hendrickson, C. L.; Jackson, G. S. Fourier Transform Ion Cyclotron Resonance Mass Spectrometry: A Primer. *Mass Spectrom. Rev.* **1998**, *17*, 1−35.
(14) Aquino-Olivos, M. A.; Andersen, S. I.; Lira-Galeana, C. Comparisons between asphaltenes from the dead and live-oil samples of the same crude oils. *Pet. Sci. Technol.* **2003**, *21* (5−6), 1017−1041.
(15) Rodgers, R. P.; Hendrickson, C. L.; Emmett, M. R.; Marshall, A. G.; Greaney, M. A.; Qian, K. Molecular Characterization of Petroporphyrins in Crude Oil by Electrospray Ionization Fourier Transform Ion Cyclotron Resonance Mass Spectrometry. *Can. J. Chem.* **2001**, *79*, 546−551.
(16) Qian, K.; Robbins, W. K.; Hughey, C. A.; Cooper, H. J.; Rodgers, R. P.; Marshall, A. G. Resolution and Identification of Elemental Compositions for More than 3000 Crude Acids in Heavy Petroleum by Negative-Ion Microelectrospray High Field Fourier Transform Ion Cyclotron Resonance Mass Spectrometry. *Energy Fuels* **2001**, *15*, 1505−1511.
(17) Qian, K.; Rodgers, R. P.; Hendrickson, C. L.; Emmett, M. R.; Marshall, A. G. Reading Chemical Fine Print: Resolution and Identification of 3000 Nitrogen-Containing Aromatic Compounds from a Single Electrospray Ionization Fourier Transform Ion Cyclotron Resonance Mass Spectrum of Heavy Petroleum Crude Oil. *Energy Fuels* **2001**, *15*, 492−498.
(18) Hughey, C. A.; Rodgers, R. P.; Marshall, A. G. Resolution of 11 000 compositionally distinct components in a single Electrospray ionization Fourier transform ion cyclotron resonance mass spectrum of crude oil. *Anal. Chem.* **2002**, *74* (16), 4145−4149.
(19) Hughey, C. A.; Rodgers, R. P.; Marshall, A. G.; Qian, K.; Robbins, W. R. Identification of Acidic NSO Compounds in Crude Oils of Different Geochemical Origins by Negative Ion Electrospray Fourier Transform Ion Cyclotron Resonance Mass Spectrometry. *Org. Geochem.* **2002,** 33, 743−759.
(20) Müller, H.; Andersson, J. T.; Schrader, W. Characterization of High-Molecular-Weight Sulfur-Containing Aromatics in Vacuum Residues Using Fourier Transform Ion Cyclotron Resonance Mass Spectrometry. *Anal. Chem.* **2005,** 77, 2536−2543.
(21) Wu, Z.; Strohm, J. J.; Song, C.; Rodgers, R. P.; Marshall, A. G. Comparative Compositional Analysis of Untreated and Hydrotreated Oil by Electrospray Ionization Fourier Transform Ion Cyclotron Resonance Mass Spectrometry. *Energy Fuels* **2005**, *19*, 1072−1077.
(22) Wu, Z.; Rodgers, R. P.; Marshall, A. G. Compositional Determination of Acidic Species in Illinois #6 Coal Extracts by Electrospray Ionization Fourier Transform Ion Cyclotron Resonance Mass Spectrometry. *Energy Fuels* **2004**, *18*, 1424−1428.
(23) Wu, Z.; Rodgers, R. P.; Marshall, A. G. Two and Three-Dimensional van Krevelen Diagrams: A Graphical Analysis Complementary to the Kendrick Mass Plot for Sorting Elemental Compositions of Complex Organic Mixtures Based on Ultrahigh-Resolution Broadband FT-ICR Mass Measurements. *Anal. Chem.* **2004**, *76*, 2511−2516.
(24) Wu, Z.; Rodgers, R. P.; Marshall, A. G. ESI FT-ICR Mass Spectral Analysis of Coal Liquefaction Products. *Fuel* **2005,** 84, 1790−1797.
(25) Marshall, A. G.; Rodgers, R. P. Petroleomics: The Next Grand Challenge for Chemical Analysis. *Acc. Chem. Res.* **2004**, *37*, 53−59.
(26) Rodgers, R. P.; Schaub, T. M.; Marshall, A. G. Petroleomics: Mass Spectrometry Returns To Its Roots. *Anal. Chem.* **2005**, 77, 20A−27A.

Table 1. Deposition and Depressurization Results for P-Drop Sample

parameter	value
bottomhole pressure	6 539 psia
initial depressurization pressure	12 000 psia
asphaltene onset pressure	4 500 psia
saturation pressure	4 000 psia
total C_7 asphaltenes in live oil sample	3.44 g
precipitated asphaltenes	0.138 g
deposited asphaltenes	0.148 g

of the oil by use of an attached bulk filtration apparatus. The asphaltenes deposited on the cell walls, the mixer, and endcap constituted the analyzed sample and are designated "P-drop asphaltenes". The results from the live oil experiments are summarized in Table 1.

Heptane-Precipitated (C_7) Asphaltenes. The C_7-insoluble asphaltenes were prepared by a modified IP-143 method.[27] The asphaltene content of the dead crude oil was 9 wt %.

Sample Preparation for ESI FT-ICR MS. Each sample (10 mg) was dissolved in 5 mL of toluene and then diluted with 5 mL of methanol to produce a final concentration of 1 mg of asphaltene per mL of solvent. Base (2 μL) was added to facilitate deprotonation for negative-ion ESI and sprayed as for positive-ion ESI.

Mass Spectrometry. Mass analysis was performed with a home-built FT-ICR mass spectrometer equipped with a 22 cm diameter horizontal bore 9.4 T actively shielded magnet (Oxford Corp., Oxney Mead, U.K.).[28] Data were collected and processed with a modular ICR data acquisition system (MIDAS).[29] Positive and negative ions were generated from a microelectrospray source equipped with a 50 μm i.d. fused silica micro-ESI needle. Samples were infused at a flow rate of 400 nL/min. Typical ESI (+) conditions were needle voltage = 2 kV and tube lens = 350 V; ESI (−) conditions were needle voltage = −2.1 kV and heated capillary current = 4 A. Ions were accumulated external to the magnet[30] in a linear octopole ion trap (25.1 cm long) equipped with axial electric field[31] for 20 s and transferred through rf-only multipoles to a 10 cm diameter, 30 cm long open cylindrical Penning ion trap. Multipoles were operated at 1.5 MHz at a peak-to-peak rf amplitude of 70 V. Broadband frequency-sweep ("chirp") dipolar excitation (70 kHz to 1.27 MHz at a sweep rate of 150 Hz/μs and a peak-to-peak amplitude, 190 V) was followed by direct-mode image current detection to yield 4 Mword time-domain data. The time-domain data were processed and Hanning-apodized, followed by a single zero-fill before fast Fourier transformation and magnitude calculation.[32] Frequency was converted to mass-to-charge ratio (m/z) by the quadrupolar electric trapping potential approximation[33,34] to generate a mass-to-charge ratio (m/z) spectrum.

Data Analysis. Mass spectra were converted from the IUPAC mass scale (based on the ^{12}C atomic mass as exactly 12 Da) to the Kendrick mass scale. The Kendrick mass scale is based on the mass of CH_2 = 14.0000 Da rather than 14.015 65 Da. Kendrick mass is obtained from the IUPAC mass as shown in eq 1.[35]

$$\text{Kendrick mass} = \text{IUPAC mass} \times (14.00000/14.01565) \quad (1)$$

Members of a homologous series (namely, compounds that contain the same heteroatom and number of rings plus double bonds but different numbers of CH_2 groups) have identical Kendrick mass defect,

$$\text{Kendrick mass defect (KMD)} = (\text{Kendrick nominal mass} - \text{Kendrick exact mass}) \quad (2)$$

and are, thus, easily sorted and selected from a list of all observed ion masses. Nominal Kendrick mass is determined by rounding up the Kendrick mass to the nearest whole number. Homologous series are then separated based on even and odd nominal Kendrick mass and KMD as described elsewhere.[36, 37]

The composition of a petroleum molecule is generally expressed by its chemical formula, $C_cH_{2c+Z}X$, in which c is the carbon number, Z is the hydrogen deficiency (measure of aromatic character), and X denotes the heteroatomic "class", namely, the constituent heteroatoms (N, S, or O) in the molecule. For convenience, we abbreviate molecular formulas according to their double bond equivalents (DBE) and heteroatomic components. Double bond equivalents are determined from eq 3.

$$\text{double bond equivalents (DBE)} = c - h/2 + n/2 + 1 \quad (3)$$

For example, pyridine is C_5H_5N, would be abbreviated as 4 N. Within the "type" (defined by DBE) and "class", 4 N, there are many compounds that differ by addition of CH_2 groups, allowing for three levels of comparisons based on type, class, and carbon number distribution.

Results and Discussion

Positive and Negative Ion ESI FT-ICR MS. Both positive- and negative-ion mass spectra were collected for the two asphaltene samples to illustrate the difference in the acidic (negative ions) and basic (positive ions) polar species. Asphaltenes are routinely detected by negative-ion electrospray and are rarely observed as positive electrosprayed ions. Here, we present a unique look at asphaltenes detected in both negative- and

(27) *Asphaltene (n-heptane insolubles) in Petroleum Products, Standards for petroleum and its Products*; Standard No. IP-143, Institute of Petroleum: London, U.K., 1985, 143.1−143.7.

(28) Senko, M. W.; Hendrickson, C. L.; Pasa-Tolic, L.; Marto, J. A.; White, F. M.; Guan, S.; Marshall, A. G. Electrospray Ionization FT-ICR Mass Spectrometry at 9.4 T. *Rapid Commun. Mass Spectrom.* **1996**, *10*, 1824−1828.

(29) Senko, M. W.; Canterbury, J. D.; Guan, S.; Marshall, A. G. A High-Performance Modular Data System for FT-ICR Mass Spectrometry. *Rapid Commun. Mass Spectrom.* **1996**, *10*, 1839−1844.

(30) Senko, M. W.; Hendrickson, C. L.; Emmett, M. R.; Shi, S. D.-H.; Marshall, A. G. External Accumulation of Ions for Enhanced Electrospray Ionization Fourier Transform Ion Cyclotron Resonance Mass Spectrometry. *J. Am. Soc. Mass Spectrom.* **1997**, *8*, 970−976.

(31) Wilcox, B. E.; Hendrickson, C. L.; Marshall, A. G. Improved ion extraction from a linear octopole ion trap: SIMION analysis and experimental demonstration. *J. Am. Soc. Mass Spectrom.* **2002**, *13* (11), 1304−1312.

(32) Marshall, A. G.; Verdun, F. R. *Fourier Transforms in NMR, Optical, and Mass Spectrometry: A User's Handbook*; Elsevier: Amsterdam, 1990; p 460.

(33) Shi, S. D.-H.; Drader, J. J.; Freitas, M. A.; Hendrickson, C. L.; Marshall, A. G. Comparison and interconversion of the two most common frequency-to-mass calibration functions for Fourier transform ion cyclotron resonance mass spectrometry. *Int. J. Mass Spectrom.* **2000**, *195/196*, 591−598.

(34) Ledford, E. B., Jr.; Rempel, D. L.; Gross, M. L. Space Charge Effects in Fourier Transform Mass Spectrometry. Mass Calibration. *Anal. Chem.* **1984**, *56*, 2744−2748.

(35) Kendrick, E. A Mass Scale Based on CH_2 = 14.0000 for High-Resolution Mass Spectrometry of Organic Compounds. *Anal. Chem.* **1963**, *35*, 2146−2154.

(36) Hsu, C. S.; Qian, K.; Chen, Y. C. An innovative approach to data analysis in hydrocarbon characterization by on-line liquid chromatography−mass spectrometry. *Anal. Chim. Acta* **1992**, *264*, 79−89.

(37) Hughey, C. A.; Hendrickson, C. L.; Rodgers, R. P.; Marshall, A. G.; Qian, K. N. Kendrick mass defect spectrum: A compact visual analysis for ultrahigh-resolution broadband mass spectra. *Anal. Chem.* **2001**, *73* (19), 4676−4681.

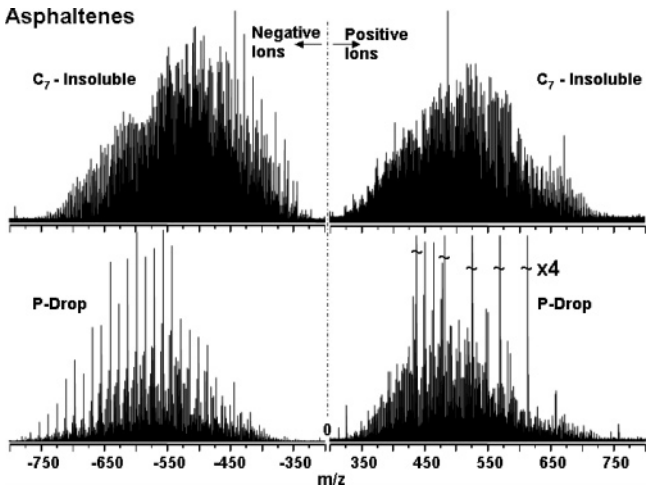

Figure 1. Broadband negative- and positive-ion electrospray ionization FT-ICR mass spectra of the C_7-insoluble and pressure-drop (P-drop) asphaltenes. All four mass spectra range from approximately 320 < m/z < 750, with little difference in the molecular weight range for the two samples. The average mass resolving power, $m/\Delta m_{50\%}$, is ~350 000 with a maximum signal-to-noise ratio of ~1000:1.

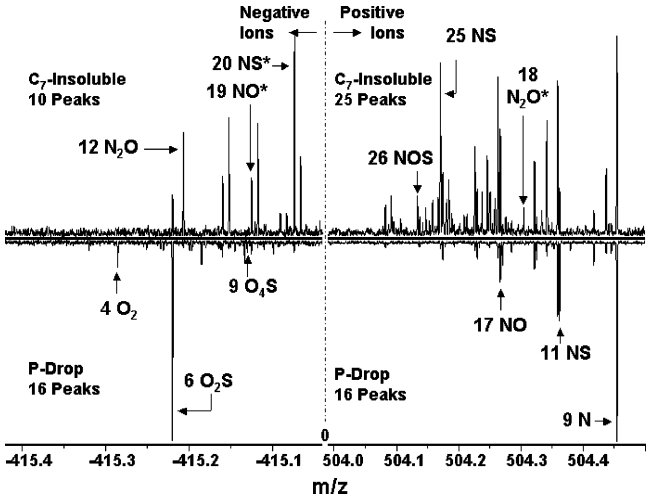

Figure 2. Mass scale-expanded segments, m/z range of ~0.5, for the C_7-insoluble (top) and P-drop (bottom, inverted) asphaltenes for positive (right) and negative (left) ions. Some of the peaks are labeled according to their "type" (DBE value) and "class" (heteroatom content). Even at this level of scrutiny, the enrichment in oxygen and sulfur heteroatoms is evident for the P-drop asphaltenes. Each * indicates the presence of one ^{13}C.

positive-ion electrospray. Analytes (including asphaltenes) are observable by positive-ion electrospray only if they contain a significant concentration of basic species. The mass spectra for C_7-insoluble and pressure-drop asphaltenes are shown in Figure 1. All four spectra exhibit an average mass resolving power, $m/\Delta m_{50\%}$, of ~400 000 at m/z 500. Elemental compositions could be assigned to approximately 12 000 peaks per sample between 300 < m/z < 750 to within ≤1 ppm error. The similarity in m/z range of the two samples for both positive and negative ions indicates similar molecular-weight distributions for the two samples.

FT-ICR MS can baseline-resolve tens of compounds per nominal mass. Figure 2 shows mass scale-expanded segments (ranging over $m/z \approx 0.5$) from all four mass spectra of Figure 1. The difference in both the number and positions of peaks clearly illustrates the differences between these two asphaltenes samples. The two samples have 4 peaks in common for both negative and positive ions. Each peak with magnitude above a

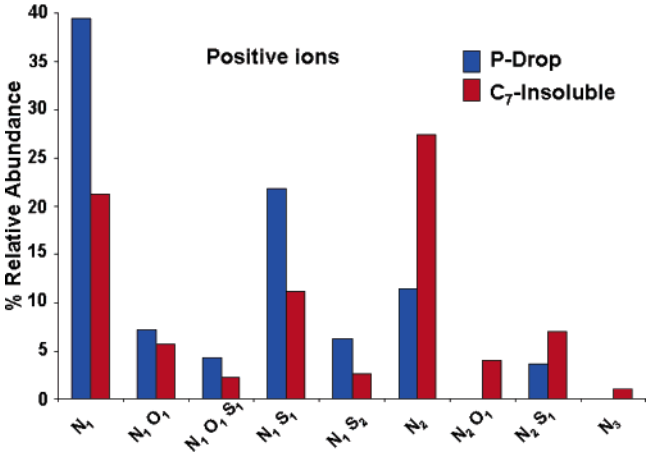

Figure 3. Compound classes for positive-ion ESI FT-ICR MS for the two asphaltene samples. Only those classes with relative abundance >1% are shown. The percent relative abundance is the summed peak heights for all species with a given heteroatom composition, divided by the summed heights for all above-threshold peaks in the spectrum. Eleven distinct heteroatom classes were observed. The P-drop asphaltenes have a somewhat higher percentage of NS-containing species and about double the relative abundance of N-containing species, whereas the C_7-insoluble asphaltenes contain a higher relative abundance of multiple-nitrogen species, such as N_2 and N_3.

threshold of 3× the standard deviation of baseline noise (3σ) is assigned an elemental composition. Each spectrum has several peaks labeled according to the double bond equivalents (DBE) and heteroatoms of its assigned elemental composition (e.g., 4 O_2). For both positive and negative ions of that nominal mass, the P-drop asphaltenes are enriched in compounds that contain both oxygen and sulfur atoms whereas the C_7-insoluble asphaltenes are composed more of compounds that contain nitrogen.

In the next two sections, we examine the similarities and differences between these two asphaltenes. First, the examination of the classes, namely, those compounds that contain the same heteroatom(s), will be compared. Both positive and negative ions will be investigated. Next, a variety of graphs will be used to compare and contrast the different types of compounds (those species that contain the same heteroatom but differ by the number of rings plus double bonds). Positive ions will be compared first, to examine the basic species that are preferentially ionized. Negative ions (acidic species) will be examined next by graphical methods, such as Kendrick plots and van Krevelen diagrams,[38,39] designed to highlight specific compositional differences.

Class Comparison. The different heteroatom classes are best visualized in simple 2D class relative abundance distributions. Class comparisons of the basic species detected as positive ions are illustrated in Figure 3. The P-drop sample displays higher abundance of species containing sulfur, such as NS and NS_2. Although the P-drop asphaltenes show higher abundance of species containing a single nitrogen atom, the C_7-insoluble asphaltenes are relatively higher in species containing multiple nitrogen heteroatoms, such as N_2 and N_3.

Negative-ion electrospray selectively ionizes acidic components: typically, carboxylic acids and pyrollic type compounds. Figure 4 shows relative abundance distributions for various heteroatom classes for negative ions from both asphaltene

(38) Kim, S.; Kramer, R. W.; Hatcher, P. G. Graphical method for analysis of ultrahigh-resolution broadband mass spectra of natural organic matter, the van Krevelen diagram. *Anal. Chem.* **2003**, *75* (20), 5336−5344.

(39) van Krevelen, D. W. Graphical-Statistical Method for the Study of Structure and Reaction Processes of Coal. *Fuel* **1950**, *29*, 269−284.

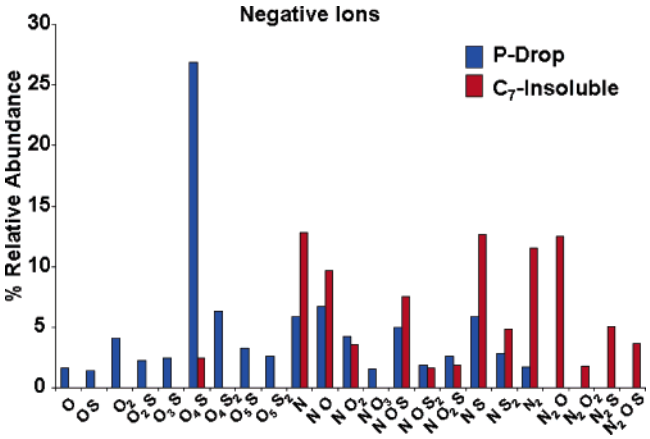

Figure 4. Compound classes in negative-ion electrospray FT-ICR MS for P-drop and C_7-insoluble asphaltenes. Only those classes with relative abundance >1% are shown. Inspection reveals an increase/presence in those compounds containing oxygen and sulfur in the P-drop asphaltenes, such as O_4S, O_2, and OS, suggesting that these species preferentially flocculate as the pressure increases. The increase/presence of those compounds containing nitrogen (such as NS, N_2S, and N_2) in the C_7-insoluble asphaltenes evidently results from their insolubility in heptane.

samples. The P-drop and C_7-insoluble asphaltenes contain 19 and 14 different heteroatom classes. The P-drop asphaltenes are dominated by classes containing both oxygen and sulfur, of which the most abundant is O_4S. In contrast, the C_7-insoluble asphaltenes are dominated by compounds that contain nitrogen, such as NS, NOS, and NO. Sulfur and oxygen heteroatoms are present only if a nitrogen atom is also present, except for relatively low abundance (~2.5%) for O_4S.

Type Comparisons. Compound type refers to the number of rings plus double bonds (DBE) associated with increasing aromaticity of a particular species. It can be graphically displayed in a Kendrick plot[37] of Kendrick mass defect (KMD) vs nominal Kendrick mass (NKM), with percent relative abundance (%RA) shown as isocontours on the third axis. Kendrick mass defect varies directly with aromaticity and, thus, provides a quick visual measure to assess aromatic character for different samples. Another graphical representation useful for highlighting type differences (specific to a single class) is a plot of double bond equivalents (DBE) vs carbon number, with signal color-coded according to percent relative abundance. Type is easily displayed along the *y*-axis along with the "carbon number" (*x*-axis) for a single class of compounds identified in the sample.

(a) Positive-Ion Electrospray. Positive-ion electrospray ionization preferentially derives from basic species such as pyridinic benzalogs. Figure 5 shows Kendrick plots for all positive ions in ESI FT-ICR mass spectra of both heptane-insoluble (C_7) and pressure-drop (P-drop) asphaltenes. The C_7-insoluble asphaltene sample has a KMD range from 0.05 to 0.50, with the most abundant species from 0.1 to 0.20, whereas the P-drop asphaltene sample KMDs range from 0.05 to 0.45, with the most abundant species from 0.05 to 0.10; the C_7-insoluble asphaltenes are, thus, more aromatic than the P-drop asphaltenes.

Close inspection of N_1 species, detected by positive ion electrospray, reveals that the heptane-insoluble (C_7-insoluble) asphaltenes have a higher abundance of species containing higher rings plus double bonds. Figure 6 shows isoabundance contours as a function of double bond equivalents and carbon number for N species (as positive ions) for both asphaltenes samples. The heptane-insoluble asphaltenes range from 4 < DBE < 32, with the highest abundance from 7 < DBE < 26. In contrast, the most abundant P-drop asphaltene N_1 species range over 10 < DBE < 12. The carbon number range for both samples is about the same, 23−52; i.e., a similar number of CH_2 groups attached to the aromatic core of each compound. Although the P-drop asphaltenes exhibit higher overall abundance of N_1 compounds, the C_7-insoluble asphaltenes have higher DBE values and are, thus, more aromatic.

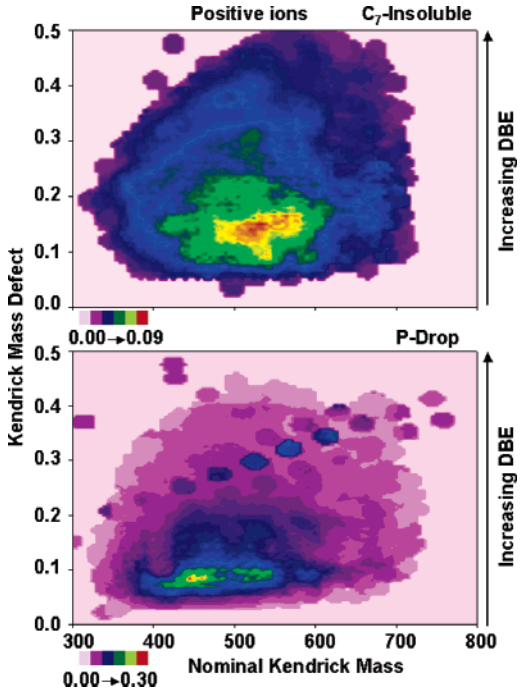

Figure 5. 3D Kendrick plot of C_7-insoluble (top) and pressure drop (bottom) asphaltenes, in which the *z*-axis (color) denotes contours of percent relative abundance of each component.

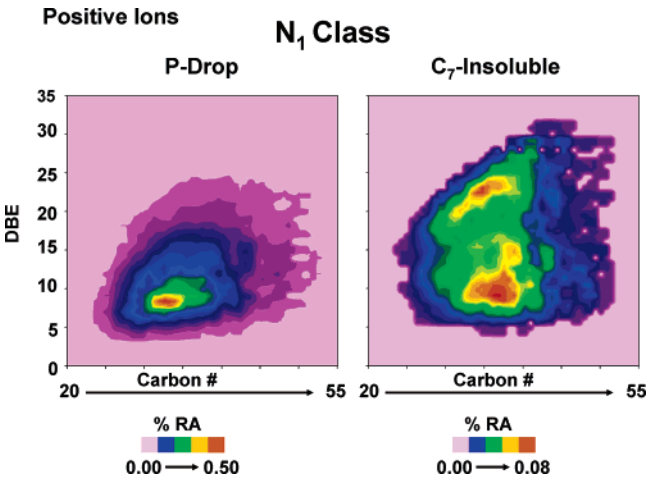

Figure 6. Double bond equivalents (DBE) vs carbon number (scaled in the third axis according to percent relative abundance contours) for positive ions that contain a single nitrogen atom. The C_7-insoluble asphaltenes have a lower %RA of single pyridine-like compounds and higher aromatic character. The most abundant species range from ~7 to 26 rings plus double bonds compared to ~10−12 rings plus double bonds in P-drop asphaltenes.

Figure 7 shows similar graphs for two additional classes of compounds detected by positive-ion electrospray. The NS class exhibits a pattern similar to that for the N_1 species, whereas the N_2 class behaves differently. Although the P-drop asphaltenes exhibit a higher overall abundance of NS compounds, the C_7-insoluble asphaltenes have higher DBE values and, thus,

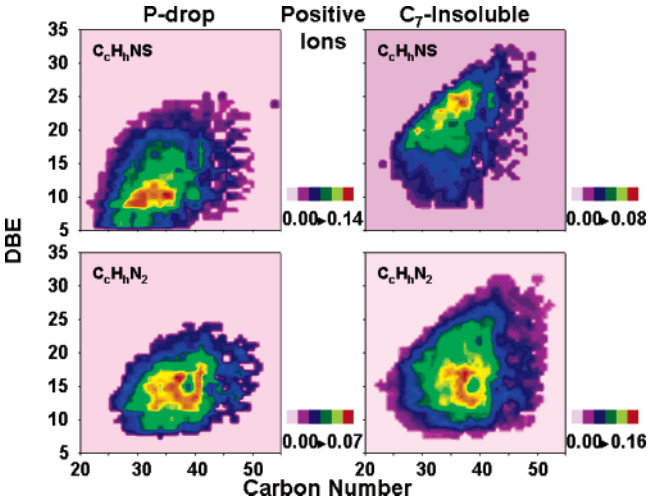

Figure 7. DBE vs carbon number (scaled in the third axis according to percent relative abundance contours) for positive ions that contain N and S heteroatoms as well as those that contain two nitrogen atoms. Those species that contain N and S follow a pattern similar to that seen in Figure 6, whereas those species that contain two nitrogen heteroatoms follow a slightly different trend.

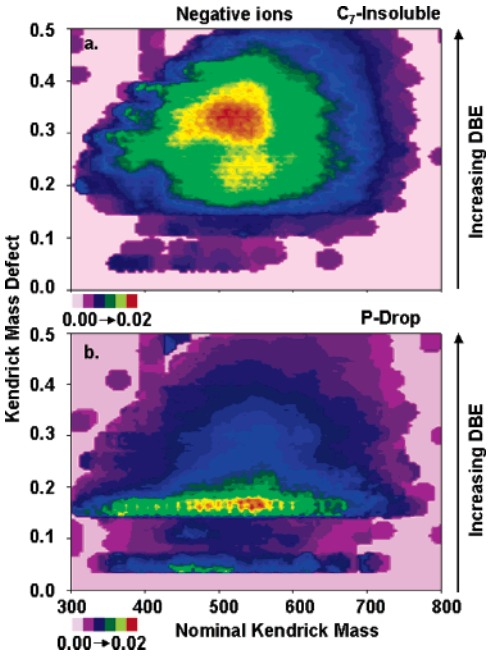

Figure 8. Kendrick mass plots of the negative ions in C_7-insoluble (top) and pressure-drop (bottom) asphaltenes. The negative ions (as for the positive ions) from the C_7-insoluble asphaltenes show more highly aromatic character than the P-drop asphaltenes. The most abundant class and type for the pressure-drop asphaltenes is 1 SO_4, with a KMD of 0.16, indicated by the green, yellow, and red colors.

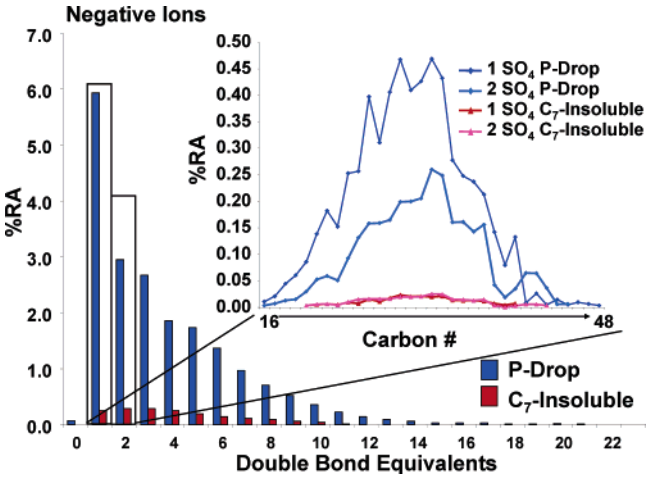

Figure 9. "Type" distribution (DBE relative abundances) for the SO_4 species of the P-drop and C_7-insoluble asphaltenes. The SO_4 series is much more abundant in the pressure-drop asphaltenes, ranging from 0 < DBE < 21, vs 1 < DBE < 11 for the C_7-insoluble asphaltenes. The carbon distributions for the two most abundant DBE types (upper right) for the pressure-drop asphaltenes is higher (i.e., more and/or longer alkyl chains) (~16−48) than that for the heptane-insoluble asphaltenes (~20−41).

contain compounds with higher aromaticity. The NS-class from the P-drop asphaltenes ranges from 6 < DBE < 25, with the most abundant species from 6 < DBE < 17, in direct contrast to the same class found in the C_7-insoluble asphaltenes, which ranges from 8 < DBE < 32, with the most abundant from 19 < DBE < 27. For both N and NS classes, the P-drop sample had a higher percent relative abundance (%RA). For the class that contains two nitrogen atoms, the C_7-insoluble asphaltenes have a higher %RA. The P-drop asphaltenes range from 8 < DBE < 24, with the most abundant between 9 and 20 rings plus double bonds. The C_7-insoluble asphaltenes range is 8 < DBE < 32, with the most abundant from 10 < DBE < 27. The difference between the two samples most likely arises from the difference in percent relative abundance of the two samples. Although both samples contain many similar classes, they do not necessarily contain similar types, as illustrated by the previous two figures.

(b) Negative-Ion Electrospray. Figure 8 shows Kendrick mass plots as in Figure 5, but for negative rather than positive ions. Negative ions derive from acidic species such as pyrollic benzalogs and carboxylic acids. The KMD range for the C_7-insoluble asphaltenes (Figure 8, top) observed as negative ions is ~0.05−0.50. The most abundant species have a KMD range from 0.2 to 0.45, indicating that the acidic species are more highly aromatic than the basic species in Figure 5. Although the overall KMD range for all species in the P-drop asphaltenes (Figure 8, bottom) is roughly the same as for the heptane-insoluble sample, the most abundant species are concentrated over a KMD range of 0.15−0.20. The highest-abundance components (KMD ≈ 0.16) are those that contain one ring or double bond, four oxygen atoms, and one sulfur atom, 1 O_4S. The shift to lower KMD indicates lower aromatic character for the P-drop asphaltenes sample.

Figure 9 compares the double bond equivalents and carbon number distributions for the O_4S class for the P-drop and C_7-insoluble asphaltenes. The DBE distributions for the two asphaltene samples are clearly very similar except for the uniformly lower relative abundance for O_4S species in the C_7-insoluble sample. The inset illustrates the carbon number distribution for O_4S class members that contain 1 or 2 rings plus double bonds. Again, the carbon number distributions are about the same, ~16−48, except for the difference in %RA (27% vs 2.5%—see Figure 4) between the two samples.

As for positive-ion electrospray, similar classes in the two asphaltene samples do *not* connote similar compound types. Figure 10 shows DBE and carbon number distributions for two classes, N and NS, found in both the P-drop and C_7-insoluble asphaltenes. Those species that contain one nitrogen heteroatom in the P-drop asphaltene have a range from 8 < DBE < 30, with the most abundant from 15 to 23 rings plus double bonds. The same class in the C_7-insoluble sample exhibits roughly the same DBE range but with the most abundant from 19 < DBE < 27, indicating a shift to higher aromatic character for the

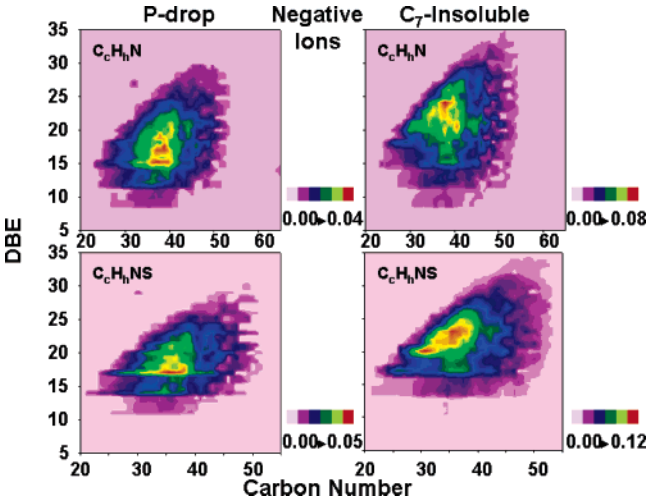

Figure 10. DBE vs carbon number (scaled in the third axis according to percent relative abundance contours) for negative ions that contain a single nitrogen atom and those that contain N and S heteroatoms.

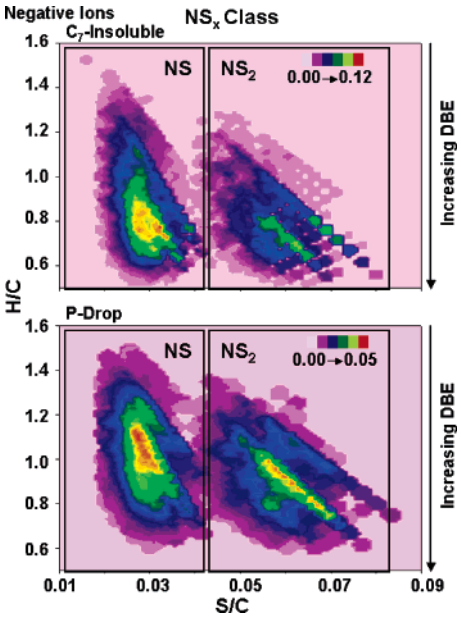

Figure 11. van Krevelen diagrams for negative ions that contain NS_x heteroatoms in the C_7-insoluble (top) and P-drop (bottom) asphaltenes. The abscissa is the ratio of sulfur atoms to carbon atoms; the ordinate is the ratio of hydrogen atoms to carbon atoms; and the third axis shows relative abundance contours. The shift to higher H/C ratio for the P-drop asphaltenes indicates lower aromatic character relative to the heptane-insolubles. The greater number of species and higher %RA of NS_2 compounds illustrates an enrichment of sulfur compounds in the P-drop asphaltenes relative to the C_7-insoluble asphaltenes.

N_1-containing class for the C_7-insoluble asphaltenes. This same trend is seen for those species that have a single nitrogen and sulfur heteroatom. Those species in the P-drop asphaltenes range from 11 < DBE < 30, whereas the same species in the C_7-insoluble asphaltenes vary from 15 < DBE < 35. This slight shift in the number of rings plus double bonds indicates the presence of higher aromatic species in the C_7-insoluble asphaltenes, as noted previously for species that contain a single nitrogen atom. The shift to a higher number of rings plus double bonds for the most abundant species within this class for the C_7-insoluble asphaltenes also indicates a shift to greater aromaticity.

Another graphical representation of crude oil type and class is a van Krevelen diagram, consisting of isoabundance contours as a function of (for example) H/C and S/C ratios for each compound containing those atoms. First conceived for bulk elemental composition,[39] the idea was first applied to all of the individual elemental compositions in humic substances by Kim et al. to distinguish condensed hydrocarbons from lipids and other components.[38] In a van Krevelen diagram, heteroatom classes may be separated on one axis (e.g., S/C ratio to distinguish classes differing in number of S atoms) and DBE differences may be spread out along the second axis (H/C ratio). A homologous alkylation series composed of compounds that contain the same number of rings plus double bonds and the same heteroatoms, but different number of CH_2 groups, shows up as diagonals. The van Krevelen allows for convenient visual separation of heteroatom class, DBE (type), and alkylation pattern.[21, 23]

van Krevelen diagrams for negative ions containing a single nitrogen atom and 1 or 2 sulfur heteroatoms are illustrated in Figure 11 for both asphaltene samples. Classes are separated along the *x* axis, and the types are separated along the *y* axis. As the H/C ratio increases, the number of rings plus double bonds decreases. There is a slight shift to lower H/C ratio (i.e., higher number of rings plus double bonds) for the C_7-insoluble asphaltenes compared to the P-drop sample. There is also an increase in the %RA of those negative ions containing two sulfur heteroatoms in the P-drop sample, consistent with the enrichment of sulfur-containing positive ions seen in Figure 3.

Conclusion

Compositional variations between asphaltenes obtained from pressure drop and C_7 precipitation are readily apparent in class and types of species identified by ESI FT-ICR MS. Interestingly, for those shared compound classes and types identified by both positive and negative ESI FT-ICR MS, the carbon number varied only slightly. Positive-ion ESI FT-ICR MS exposes compositional differences in the basic species and shows that the C_7 asphaltene sample contains lower relative abundance of the N_1-containing species but is higher in rings plus double bonds compared to the P-drop asphaltenes. The pressure-drop asphaltenes are enriched in compounds that contain sulfur, such at NS and NS_2, with fewer rings plus double bonds compared to the C_7 asphaltenes. Negative-ion ESI FT-ICR MS exposes compositional differences in the acidic species, revealing the enrichment of oxygen- and sulfur-containing species in the pressure-drop sample. As for the aromaticity differences seen in the basic species, the pressure-drop sample is composed of less aromatic, heteroatom-containing compounds compared to the C_7 asphaltene sample. The analysis of dead-oil asphaltenes may, thus, be very misleading, because if the oil loses material upon pressure reduction, then only a subset of the asphaltene fraction remains in the dead oil. On the basis of this study, that subset is quite different in composition than its corresponding depressurization asphaltene. Depressurization favors the flocculation of low-DBE, highly-polar species that comprise O_xS (*x* is any integer, 2−5), O_2, NS, NS_2, and O_4S_2 classes. The analysis of crude oil components by ESI FT-ICR MS opens the door to compound-specific comparison between crude oils—namely, the backbone of petroleomics. The ability to baseline-resolve and assign elemental compositions at a molecular level allows us to not only study crude oils at an unprecedented level of detail but also potentially predict production behavior involving asphaltene-like compounds. On the basis of the present results, it is clear that asphaltenes obtained from live and dead oils show clear compositional differences. Therefore, severe caution must be used in attempting to predict production performance based

on bulk solvent drop asphaltenes. Live oil samples provide the greatest insight into potential crude oil asphaltene production issues.

Acknowledgment. The authors thank Christopher L. Hendrickson and John P. Quinn for helpful discussions and Daniel McIntosh for machining all of the custom parts required for the 9.4 T instrument construction. This work was supported by the NSF National High Field Mass Spectrometry Facility (DMR 00-84173), Florida State University, and the National High Magnetic Field Laboratory in Tallahassee, FL.

EF0600199